Conclusions

The separation bubble developed on an airfoil surface is successfully calculated using a PPNS procedure with the boundary condition that is free of bubble influences. Inclusion of the higher-order curvature terms in the equations, in combination with the proper outer boundary condition, is found necessary to get the desired results.

Acknowledgments

This work was supported by the Korea Science and Engineering Foundation. The authors are grateful to the reviewers for their valuable comments.

References

[1]Briley, W. R. and McDonald, H., "Numerical Prediction of Incompressible Separation Bubbles," *Journal of Fluid Mechanics,* Vol. 69, Pt. 4, June 1975, pp. 631-656.

[2]Cebeci, T. and Schimke, S. M., "The Calculation of Separation Bubbles in Interactive Tubulent Boundary Layers," *Journal of Fluid Mechanics,* Vol. 131, June 1983, pp. 305-317.

[3]Vatsa. V. N. and Carter, J. E., "Analysis of Airfoil Leading Edge Separation Bubbles," *AIAA Journal,* Vol. 22, Dec. 1984, pp. 1697-1704.

[4]Kwon, O. K. and Pletcher, R. H., "Prediction of Subsonic Separation Bubble on Airfoils by Viscous-Inviscid Interaction," *Proceedings of a Symposium on Numerical and Physical Aspects of Aerodynamic Flows III,* edited by T. Cebeci, Springer-Verlag, New York, 1984, pp. 163-171.

[5]York, B. and Knight, D., "Calculation of Two-Dimensional Turbulent Boundary Layers Using the Baldwin-Lomax Model," *AIAA Journal,* Vol. 23, Dec. 1985, pp. 1849-1850.

[6]Galpin, P. F., Van Doormaal, J. P., and Raithby, G. D., "Solution of the Incompressible Mass and Momentum Equations by Application of a Coupled Equation Line Solver," *International Journal of Numerical Methods in Fluids,* Vol. 5, July 1985, pp. 615-625.

[7]Gault, D. E., "An Experimental Investigation of Regions of Separated Laminar Flow," NACA TN 3505, Sept. 1955.

Evaluation of the Gradient Model of Turbulent Transport Through Direct Lagrangian Simulation

Peter S. Bernard* and Mohamed F. Ashmawey†
University of Maryland, College Park, Maryland
and
Robert A. Handler‡
Naval Research Laboratory, Washington, D.C.

Introduction

THE mean gradient, or eddy viscosity, model of momentum transport has been an essential component of a wide range of closure schemes.[1] Many of these have achieved some significant successes, particularly in the prediction of relatively simple shear flows such as those in channels, pipes, or nonseparating boundary layers. In spite of these accomplishments, substantial questions remain concerning the fundamental validity of the approach. Criticisms of the gradient law extend back at least to Taylor,[2,3] who thought that its basic premise, that momentum would be conserved on particle paths over a mixing length, failed to account realistically for the likely effect that pressure forces would have on the motion of fluid particles. Later Corrsin[4] showed that the circumstances under which gradient transport could be trusted are more restrictive than the conditions usually found in practice. In particular, the length scale of turbulent mixing is often comparable to that over which the gradient field varies. A detailed analysis of gradient transport also has been provided by Tennekes and Lumley,[5] who have pointed out its incompatibility with the accepted belief that Reynolds stress is produced mostly in coherent events involving vortical structures.

The limitations of the eddy viscosity model appear to surface more clearly in the case of complex flows,[6] where the level of performance of many closure schemes depending on it has been less than satisfactory. Presumably, in this instance essential nongradient processes in the physics of turbulent transport cannot be neglected. A well-known example of this is the wall jet flow,[7] where the gradient model is fundamentally at odds with the observed mean velocity and Reynolds shear stress fields.

To date, previous analyses of turbulent momentum transport have had to rely, in varying degrees, on heuristic arguments, since the Reynolds stress does not lend itself readily to formal treatment by the usual statistical techniques. It is of some interest, therefore, to develop a method of testing the gradient transport hypothesis that is purely formal, i.e., involving no assumptions.

In this Note, a Lagrangian expansion of the Reynolds shear stress is introduced that, in principle, allows for a precise test of the gradient transport model. An analogous construction for the case of vorticity transport has been used previously in developing closure schemes.[8-10] The implementation of this analysis requires evaluation of the terms in the expansion by ensemble averaging over a data file of Lagrangian particle paths. For the present study the necessary paths were obtained at two locations near the boundary from a direct numerical simulation of turbulent channel flow.[11] The results confirm that the most significant source of nongradient transport arises from the influence of the pressure field. Of somewhat less importance, but significant nonetheless, are higher-order effects originating from transport on a scale greater than that of linear variation in mean velocity.

Analysis of Gradient Transport

It is desirable to explain the source of correlation in $\overline{uv}$ at a particular point $\boldsymbol{a}$ at time t_0. Here and henceforth, u, v, and w represent the streamwise, wall-normal, and spanwise velocity fluctuations, respectively, in a channel flow; $\overline{U}$ is the mean streamwise velocity, $U = \overline{U} + u$, and the overbar denotes an ensemble average. Consider a fluid particle with trajectory $\boldsymbol{x}(\boldsymbol{a},t)$ that is known to be at point $\boldsymbol{a}$ at time t_0, i.e., $\boldsymbol{x}(\boldsymbol{a},t_0) = \boldsymbol{a}$. Henceforth, the given point $(\boldsymbol{a},t_0)$ will be denoted as point $\boldsymbol{a}$ while the position occuring earlier in time along the path, at $t = t_0 - \tau, \tau > 0$, is denoted as point b. In contrast to point $\boldsymbol{a}$, point b varies randomly from realization to realization of the turbulent field.

Integration of the U component of the Navier-Stokes equation along $\boldsymbol{x}(\boldsymbol{a},t)$ from b to $\boldsymbol{a}$ yields

$$U_a - U_b = -\int_{t_0-\tau}^{t_0} \nabla p \, ds + \int_{t_0-\tau}^{t_0} \frac{1}{R} \nabla^2 U \, ds \qquad (1)$$

which indicates that the momentum of the fluid particle changes along the path due to the accumulated action of the pressure and viscous forces. Here R is an appropriate Reynolds number, p is the nondimensional pressure field, and subscripts $\boldsymbol{a}$ and b denote quantities evaluated at points $\boldsymbol{a}$ and b, respectively.

Expressions U_a and U_b in Eq. (1) may be decomposed into $U_a = \overline{U}_a + u_a$ and $U_b = \overline{U}_b + u_b$, where it should be noted

Received June 22, 1988; revision received Dec. 20, 1988.

*Associate Professor, Department of Mechanical Engineering.

†Graduate Research Assistant, Department of Mechanical Engineering.

‡Research Engineer, Laboratory for Computational Physics and Fluid Dynamics.

that $\bar{U}_b$ and u_b represent their respective Eulerian fields evaluated at the random point b. It will be useful in later analysis to introduce Lagrangian correlation functions such as $R_{uu}(-\tau) = \overline{u_a u_b}$. Functions R_{vv}, R_{ww}, R_{uv}, and R_{vu} may be similarly defined. With these definitions it follows from Eq. (1) that

$$\overline{u_a v_a} = R_{vu}(-\tau) + \overline{v_a(\bar{U}_b - \bar{U}_a)} + \Phi_1 \tag{2}$$

where Φ_1 is the correlation of the integral terms in Eq. (1) with v_a. The first two terms on the right-hand side of Eq. (2) can be evaluated directly from an ensemble of particle paths computed from a direct numerical simulation of channel flow. Since $\overline{u_a v_a}$ is also known, Φ_1 can be computed as the closing entry. In this way a decomposition of $\overline{uv}$ into computable factors is possible.

The second term on the right-hand side of Eq. (2) represents the correlation of v_a with the change in the mean velocity field between points b and a. This term will potentially contribute to a gradient transport law since the sign of the difference, $(\bar{U}_b - \bar{U}_a)$, is selected from up or down the $\bar{U}$ gradient depending on the sign of v_a. For the case of channel flow, the Taylor series expansion of $\bar{U}_b$ about point a consists of

$$\bar{U}_b = \bar{U}_a - \int_{-\tau}^{0} v(s)\, ds \frac{d\bar{U}}{dy}(a) + \mathcal{O}(\tau^2)$$

in which $\int_{-\tau}^{0} v(s)\, ds$ is the wall-normal displacement of a fluid particle from point b to a. From this relation it follows that

$$\overline{v_a(\bar{U}_b - \bar{U}_a)} = -\int_{-\tau}^{0} R_{vv}(s)\, ds \frac{d\bar{U}}{dy}(a) + \Phi_2 \tag{3}$$

Here Φ_2 is the correlation of v_a with terms of $\mathcal{O}(\tau^2)$ appearing in the Taylor series expansion of $\bar{U}_b - \bar{U}_a$. The first term on the right-hand side of Eq. (3) can be evaluated from the particle path data, as can the left-hand side, so that Φ_2 can be obtained as the closing entry.

Substituting Eq. (3) into Eq. (2) and rearranging yields

$$\overline{uv} = -\int_{-\tau}^{0} R_{vv}(s)\, ds \frac{d\bar{U}}{dy} + R_{vu}(-\tau) + \Phi_1 + \Phi_2 \tag{4}$$

where evaluation of appropriate quantities at point a is to be understood. This relation holds for all values of τ. In particular, it may be observed that Eq. (4) will reduce to a gradient transport law on the condition that a value of τ exists for which the last three terms are negligible. The most likely scenario under which this can occur, assuming terms Φ_1 and Φ_2 are small, is for the eddy diffusivity $\int_{-\tau}^{0} R_{vv}(s)\, ds$ in Eq. (4) to converge for large enough τ to Tv^2, where $T \equiv \int_{-\infty}^{0} R^*_{vu}(s)\, ds$ is the Lagrangian integral scale, while simultaneously the correlation $R_{vu}(-\tau)$ becomes zero. Here and henceforth, $R^*_{vv}(s)$ refers to the normalized correlation $R_{vv}(s)/R_{vv}(0)$.

Since Φ_2 depends on terms of $\mathcal{O}(\tau^2)$, it is likely that τ must be bounded from above for this term to be small. Expression Φ_1, on the other hand, being $\mathcal{O}(\tau)$, can only be small if the underlying correlation is weak. It is precisely the effect represented by this term, particularly as regards the pressure,[2,3] that has long been held as a chief source of nongradient transport. In summary, it may be expected that the validity of the gradient model rests largely on the magnitude of Φ_1, in addition to whether or not a value of τ exists for which both the second and fourth terms on the right-hand side of Eq. (4) are simultaneously negligible.

In the preceding discussion the assumption was made that $\tau > 0$ so that a backward analysis was implied. It may be shown, however, that Eq. (4) applies equally well in the event that $\tau < 0$. In this case a collection of forwardly tracked particles is needed to evaluate the terms in the expansion. Inspection of the gradient term in Eq. (4) reveals that there is, in fact, a fundamental difference between a backward and forward analysis of $\overline{uv}$. In particular, the eddy viscosity $\int_{-\tau}^{0} R^*_{vv}(s)\, ds$ in Eq. (4) is positive for $\tau > 0$, yet negative for $\tau < 0$. In other words, $\overline{uv}$ and the gradient term in Eq. (4) will always have opposite signs, so that a forward momentum analysis cannot yield a useful result. This appears to conform to one's intuition that the existence of a correlation between u and v at a particular point in space and time can only be explained by

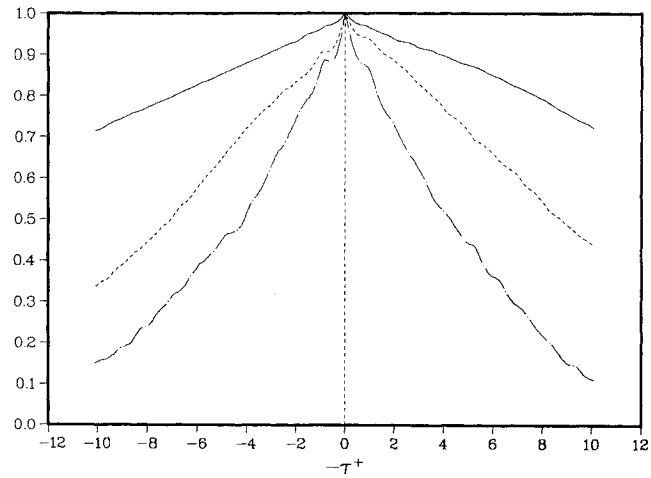

Fig. 1 Ensemble-averaged correlations: R^*_{uu}, ——; R^*_{vv}, — · — · —; and R^*_{ww}, -------.

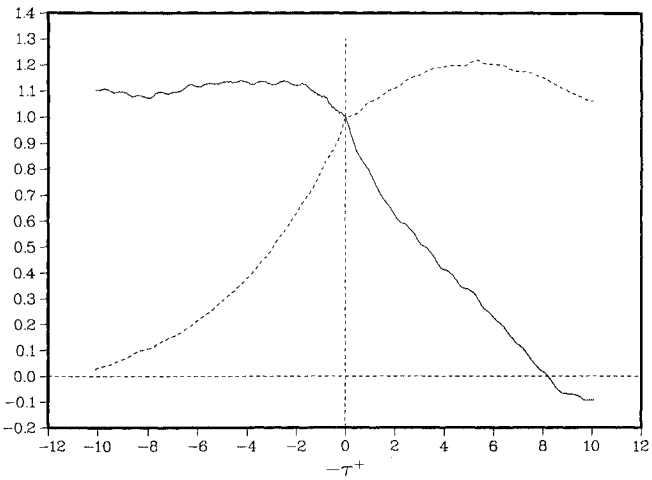

Fig. 2 Ensemble-averaged correlations: R^*_{uv}, —— and R^*_{vu}, --------.

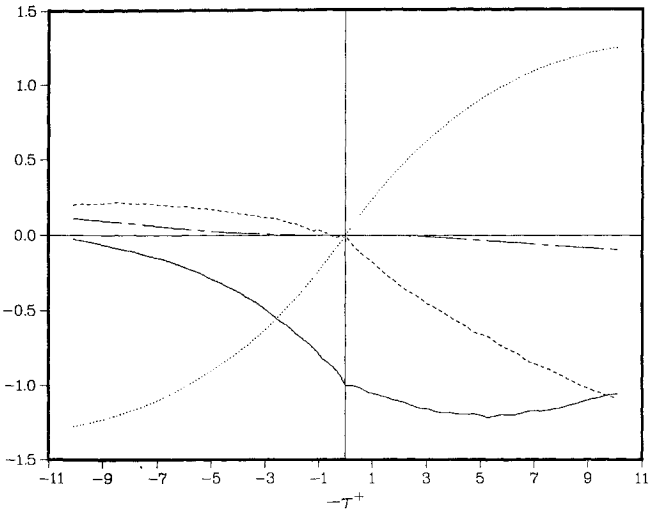

Fig. 3 Computed terms in Eq. (4) normalized by $|\overline{uv}|$: gradient term, · · · · · · ·; R_{vu}, ——; Φ_1, ---------; and Φ_2, — · — · —.

examining the past history of the turbulent flow and not by looking into its future motion.

Numerical Results

A collection of particle paths with which to evaluate the terms in Eq. (4) was obtained from a direct numerical simulation of turbulent channel flow[11] at Reynolds number $R^* = 173.2$ based on friction velocity and half-channel width. From initial locations on each of the planes $y^+ = 15.8$ and 37.5, 801 particles were followed forward in time. The total elapsed time of the simulation was $T^+ = 10$, which required 280 time steps to achieve. In the present discussion, y^+, T^+, and τ^+ refer to quantities scaled by wall variables. Each of the 280 calculated velocity fields was stored on magnetic tape so that backward paths could be computed. In this case, 601 particles were followed backward in time from each of the same two starting planes at $y^+ = 15.8$ and 37.5.

Ten randomly selected particles were followed forward and backward 280 time steps as a test of the accuracy of the computed paths. On average, the particles returned to within a very small distance, $d^+ \approx 0.44$, of their initial positions. Thus, the ensemble of computed paths appeared to be of sufficient accuracy to be used in the transport analysis. Additional details concerning the path data may be found in Ref. 12.

Figure 1 displays the normalized correlation functions R^*_{uu}, R^*_{vv}, and R^*_{ww} at $y^+ = 15.8$, while R^*_{uv} and R^*_{vu} are given in Fig. 2. The abscissa in all figures is taken as $-\tau^+$, so the curves to the left of the origin represent a backward analysis and those to the right a forward analysis. The curves for R^*_{vv} in Fig. 1 and R^*_{vu} in Fig. 2 are relevant to the evaluation of Eq. (4). For both positive and negative $-\tau^+$, R^*_{vv} falls relatively close to zero by $T^+ \approx 10$. On the other hand, only for $-\tau^+ < 0$ does R^*_{vu} approach zero. In fact, for $-\tau^+ > 0$, R^*_{vu} increases to values greater than one before eventually decreasing. This asymmetry is not unlike that observed in similar two-point Eulerian correlation functions.[13] It also complements the asymmetry of the gradient term in Eq. (4) mentioned previously. This is made clear in Fig. 3, which contains a plot of the computed terms in Eq. (4) normalized by $|\overline{uv}|$ at $\tau^+ = 0$. Note that at any time the four curves must sum to -1 and that the second term on the right-hand side of Eq. (4) is now given by $-R^*_{vu}$. For $-\tau^+ < 0$, the increase in $-R^*_{vu}$ from -1 toward zero coincides with a decrease in the gradient term; i.e., in the figure the gradient term decreases from 0 toward -1. The opposite effect occurs for $-\tau^+ > 0$, whererin the gradient term becomes positive while $-R^*_{vu}$ decreases below -1. This verifies that only a backward analysis of transport is useful.

The curve for Φ_2 in Fig. 3 is virtually zero for $|\tau^+| \leq 3$, strongly confirming the analysis leading to Eq. (3). For $|\tau^+| > 3$, second-order effects begin to mount. By $-\tau^+ \approx -10$, when $-R^*_{vu} \approx 0$, the normalized $\Phi_2 \approx 0.1$. Thus, the aforementioned requirement that a value of τ^+ exists for which the terms R_{vu} and Φ_2 are both small does not appear to be met. However, the 10% discrepancy to a gradient law introduced by the higher-order terms does not appear to be too serious.

It is seen in Fig. 3 that Φ_1 is a source of significant nongradient effects. At $-\tau^+ \approx -10$ its magnitude is 20% of the Reynolds stress. Since it has the same sign as Φ_2, the influence of these two sources of nongradient transport is additive. As a result, a purely gradient transport law appears to be in error by approximately 30% at $y^+ = 15.8$. Very similar trends to those shown in Figs. 1-3 were observed at $y^+ = 37.5$, though in this case the total simulation time was not long enough to bring R^*_{vu} as close to zero as it is in the $y^+ = 15.8$ case.

The present study reaffirms the need to develop Reynolds stress models that take into account important nongradient transport phenomena. One approach to this end is to work indirectly through vorticity transport modeling, where no pressure effects explicitly appear. Some preliminary steps in this direction have been taken[9] in which a Lagrangian analysis has been employed. A test of these results using particle path data as used in the present study is planned.

Acknowledgments

Support of P. S. Bernard for this study was provided in part through an American Society for Engineering Education/ Navy Summer Faculty Research Fellowship.

References

[1]Reynolds, W. C., "Computation of Turbulent Flows," *Annual Review of Fluid Mechanics*, Vol. 8, 1976, pp. 183-208.

[2]Taylor, G. I., "Eddy Motion in the Atmosphere," *Philosophical Transactions of the Royal Society*, Vol. 215, 1915, pp. 1-26.

[3]Taylor, G. I., "The Transport of Vorticity and Heat Through Fluids in Turbulent Motion," *Proceedings of the Royal Society*, Vol. 135A, 1932, pp. 685-705.

[4]Corrsin, S., "Limitations of Gradient Transport Models in Random Walks and Turbulence," *Advances in Geophysics*, Vol. 18A, 1974, pp. 25-60.

[5]Tennekes, J. and Lumley, J. L., *A First Course in Turbulence*, MIT, Cambridge, MA, 1972.

[6]Lakshminarayama, B., "Turbulence Modeling For Complex Shear Flows," *AIAA Journal*, Vol. 24, Dec. 1986, pp. 1900-1917.

[7]Hinze, J. O., *Turbulence*, 2nd ed., McGraw-Hill, New York, 1975, p. 580.

[8]Bernard, P. S. and Berger B. S., "A Method for Computing Three-Dimensional Turbulent Flows," *SIAM Journal on Applied Mathematics*, Vol. 42, June 1982, pp. 453-470.

[9]Bernard, P. S., "Non-Gradient Transport Phenomena in Turbulent Shear Flows," *Proceedings First National Fluid Dynamics Congress*, AIAA, Washington, DC, 1988, pp. 553-557 (AIAA Paper 88-3749-CP).

[10]Rhines, P. B. and Holland, W. R., "A Theoretical Discussion of Eddy-Driven Mean Flows," *Dynamics of Atmospheres of Oceans*, Vol. 3, July 1979, pp. 289-325.

[11]Hansen, R. J., Handler, R. A., Leighton, R. I., and Orszag, S. A., "Prediction of Turbulence-Induced Forces on Structures from Full Numerical Solutions of the Navier-Stokes Equations," *Journal of Fluids and Structures*, Vol. 1, Oct. 1987, pp. 431-443.

[12]Bernard, P. S., Ashmawey, M F., and Handler, R. A., "An Analysis of Particle Trajectories in Computer Simulated Turbulent Channel Flow," *Proceedings of the Eleventh Symposium on Turbulence,* Univ. Missouri, Rolla, MO, 1988.

[13]Antonia, R. A. and Van Atta, C. W., "Statistical Characteristics of Reynolds Stresses in a Turbulent Boundary Layer," *AIAA Journal*, Vol. 15, Jan. 1977, pp. 71-75.

Steady, Shock-Capturing Method Applied to One-Dimensional Nozzle Flow

S. Parameswaran*
Texas Tech University, Lubbock, Texas

Introduction

UPWIND difference schemes are becoming increasingly popular for the solution of the Euler equations because they are compatible with the characteristic theory (see Refs. 1-3). In the present method, the steady Euler equations are modeled by an upwind difference scheme and solved by a modified version of the SIMPLE algorithm originally developed for steady, incompressible flows by Patankar and Spalding.[4]

Received March 22, 1988; revision received Dec. 20, 1988.

*Visiting Assistant Professor, Department of Mechanical Engineering.